Article | Received 26 May 2025; Revised 25 August 2025; Accepted 18 September 2025; Published 30 September 2025
https://doi.org/10.55092/aias20250007

Passenger motion sickness binary classification model and analysis of vehicle lighting intervention effect

Bin Ren*, Xiaoyuchen Wang, Pengyu Ren and Menghan Wu

Shanghai Key Laboratory of Intelligent Manufacturing and Robotics, School of Mechatronic Engineering and Automation, Shanghai University, Shanghai 200444, China

* Correspondence author; E-mail: binren@i.shu.edu.cn.

Highlights:

- We systematically evaluated the effects of different lighting conditions on passenger motion sickness in real driving scenarios to verify the mitigating effect of red light on passenger motion sickness.
- We analyzed passengers' brain activities and cardiovascular responses under different lighting conditions to reveal the potential role of lighting on motion sickness relief and its physiological mechanisms based on multimodal physiological datasets.
- We constructed and validated a deep learning fusion binary classification model, which integrated temporal convolutional, spatial convolutional, and multi-head attention mechanisms for accurate real-time motion sickness detection.

Abstract: This study investigated the effects of ambient lighting on passenger motion sickness during real-world nighttime driving. Motion sickness was assessed through subjective ratings and simultaneous EEG-ECG recordings. The binary classification model was proposed to optimize passenger comfort and tested in the intelligent cabin for Feifan F7 series electric vehicle of Shanghai Automotive Industry Corp（SAIC）. The lighting conditions was tested for three volunteers: warm red light (620–650 nm), cool blue light (450–470 nm), and no-light. Results showed significant differences across conditions, with red light demonstrating the strongest protective effect, no motion sickness 77.8% red light *vs.* 38.9% blue light and 27.8% no light. Red light significantly enhanced alpha power and reduced delta power, suggesting neurological relaxation. Therefore, a comprehensive validation of wavelength-specific lighting effects on automotive motion sickness was completed, demonstrating that warm red light effectively mitigates symptoms through enhanced alpha wave activity.

Keywords: motion sickness; ambient lighting intervention; EEG-ECG fusion; deep learning classification; intelligent cabin comfort; Shanghai Automotive Industry Corp（SAIC）

1. Introduction

Motion sickness is a typical physiological response triggered by inconsistent information from visual, vestibular, and proprioceptive systems, which is characterized by discomfort such as nausea, dizziness,

and vomiting [1–3]. This sensory conflict phenomenon has a high incidence in the population, and epidemiologic surveys have shown that about two-thirds of individuals have experienced motion sickness [4–6]. With the rapid development of the automotive industry and the wide application of intelligent driving technology, the impact of in-vehicle motion sickness on passenger comfort and driving safety has become increasingly prominent. Especially in the nighttime driving environment, the significant reduction of external visual references and the relatively closed spatial characteristics of the cabin further exacerbate the information conflict between multisensory systems, which leads to the worsening of motion sickness symptoms [7,8]. This phenomenon not only directly impairs passengers' travel comfort experience but also may negatively affect driving behavior due to distraction or physical discomfort, constituting a potential traffic safety hazard.

The environmental factors including lighting system could significantly modulate the degree of motion sickness by regulating passengers' physiological state and psychological perception [9]. The in-vehicle lighting system, as a highly controllable environmental variable whose spectral characteristics (color temperature) and light intensity parameters have a significant impact on human visual perception, vestibular balance system, and autonomic nervous system functions, has shown great potential for application in the alleviation of motion sickness symptoms [10,11]. Therefore, in-depth exploration and development of environmental intervention-based motion sickness mitigation strategies are of great theoretical value and practical significance for optimizing automobile user experience and protecting driving safety.

The environmental factors have a significant effect on motion sickness, such as lighting, temperature, which modulate motion sickness by influencing passengers' physiological and psychological states. The interior lighting as a controllable environmental variable plays a potential role in motion sickness mitigation because its color temperature and brightness significantly affect visual perception, the vestibular system, and the autonomic nervous system [12]. Hainich *et al.* developed a Human Machine Interface (HMI) utilized ambient light cues to mitigate motion sickness in self-driving vehicles [13]. However, not all light types are beneficial for alleviating motion sickness. Kim K *et al.* found that nausea scores were significantly higher ($P < 0.01$) in subjects after exposure to blue light compared to green light (mid-wavelength, 555 nm), suggesting that short-wavelength light may aggravate the symptoms of motion sickness through the stimulation of the visual system and exacerbation of sensory conflict [14]. Regarding neurophysiological mechanisms, short-wavelength blue light (450–470 nm) has been shown to activate retinal intrinsic photosensitive ganglion cells (ipRGCs), leading to enhanced sympathetic nervous system activity, which may exacerbate motion sickness symptoms [15]. In contrast, long-wavelength red light (620–650 nm) promotes parasympathetic nervous system activity, potentially reducing the neurological stress response associated with motion sickness [16]. Mao Y *et al.* found that stroboscopic light (SSL) synchronized with motion effectively alleviated symptoms of motion sickness induced by passive motion by inhibiting vestibular-autonomic pathways [17].

Electroencephalogram (EEG) signals have become a core physiological indicator of the central nervous system's response to motion sickness, with the power of specific frequency bands showing highly consistent correlations with the degree of motion sickness discomfort. Henry E *et al.* conducted an EEG recording study in a real driving environment. They systematically elucidated the pattern of changes in electroencephalographic (EEG) activity during motion sickness, emphasizing significant correlations between changes in neuronal rhythms in occipital and parietal regions and the integration

of sensory information and the progression of motion sickness symptoms [18]. The important correlation between the electrocardiogram (ECG) and other physiologic indices is also significant in assessing motion sickness. The heart rate variability (HRV) parameter can effectively reflect the functional changes of the autonomic nervous system during motion sickness, providing important additional information for understanding the physiological mechanisms of motion sickness. In addition, integrating and applying multidimensional physiological indicators, such as thermoregulation and galvanic skin response, further enriched the basis for constructing an objective assessment system.

With the rapid development of artificial intelligence technology, machine learning methods show great potential in motion sickness recognition and prediction. Li C *et al.* constructed a multidimensional physiological feature assessment model based on electrogastrogram, facial skin color change, temperature fluctuation, and nystagmus indicators. They achieved a classification accuracy of 88.24% using the support vector machine (SVM) algorithm, significantly exceeding the performance of the traditional subjective assessment method [19]. Keshavarz B *et al.*, on the other hand, focused on developing real-time recognition technology for visually induced motion sickness (VIMS) [20]. By systematically integrating multiple physiological indicators with advanced machine learning algorithms, they found that changes in facial skin temperature and body movement patterns had the strongest correlation with VIMS symptoms, which provided an important technological pathway to developing a real-time motion sickness monitoring system.

Considering the significant individual variability of motion sickness responses, individualized modeling approaches have gradually gained attention. Irmak T *et al.* developed an individualized motion sickness prediction model based on visual environmental features, which not only verified the decisive influence of visual factors on motion sickness symptoms but also confirmed the high reproducibility of individual physiological response patterns and highlighted the physiological indicators such as galvanic skin conductance responses (GSRs) in an individualized assessment of the application value [21].

In order to explore the effects of different ambient lights (no light, cool blue light, and warm red light) on the degree of motion sickness of passengers in a nighttime in-vehicle environment we assessed the motion sickness responses under each lighting condition through non-invasive physiological monitoring techniques.

(1) Using the Feifan F7 series electric vehicle of SAIC, we systematically evaluated the effects of different lighting conditions on passenger motion sickness in real driving scenarios and verify the mitigating effect of red light on passenger motion sickness. Adaptive lighting intervention strategies that can be integrated into intelligent vehicle cockpit environments are also proposed to provide theoretical and technical support for developing next-generation passenger comfort systems.

(2) We constructed and validated a deep learning binary classification model based on EEG-ECG fusion, which integrates temporal convolutional, spatial convolutional, and multi-head attention mechanisms for accurate real-time motion sickness detection.

(3) Combining multimodal physiological data such as electroencephalogram (EEG) and electrocardiogram (ECG), we analyzed passengers' brain activities and cardiovascular responses under different lighting conditions to reveal the potential role of lighting on motion sickness relief and its physiological mechanisms.

By combining multimodal physiological datasets such as electroencephalogram (EEG) and electrocardiogram (ECG) to analyze passengers' brain activity and cardiovascular response under different

lighting conditions, we could reveal the potential role of lighting on motion sickness relief and its physiological mechanisms.

In the nighttime test of the electric vehicle, the effects of dim light, blue light, and red light on passengers' motion sickness were compared, and a fusion binary classification model was constructed using EEG and ECG signals to reveal the neural mechanism of lighting intervention.

2. A binary classification model for motion sickness

Motion sickness involved the synergistic effects of multiple physiological systems: EEG signals reflect brain activity, e.g., Delta wave power enhancement was associated with discomfort; ECG signals reveal autonomic responses, e.g., elevated low frequency/high frequency (LF/HF) ratios were correlated with sympathetic excitation.

Traditional machine learning methods cannot effectively capture the spatio-temporal dynamic features of EEG and ECG signals when processing them. Standard convolutional neural networks (CNNs) had the following limitations in processing such signals: the temporal dynamics and inter-channel spatial correlation of EEG signals need to be modeled separately. The standard CNNs had difficulty in processing these two types of features simultaneously. The features of EEG and ECG signals need to be effectively aligned in both temporal and spatial dimensions, and traditional methods had difficulty in achieving efficient fusion. Therefore, the motion sickness-related features could be concentrated in specific periods or channels, and standard CNNs cannot focus on key features selectively.

In order to investigate the effect of lighting intervention on motion sickness status, this study constructed an end-to-end binary classification model based on the fusion of raw EEG and ECG signals. The model takes raw physiological signals as direct input without requiring manual feature extraction or preprocessing, enabling automatic feature learning throughout the entire pipeline. Through the temporal convolution module (TCM), spatial convolution module (SCM), and attentional mechanism module (AM), the model extracted the temporal dynamic features, spatial correlation features, and key feature weights of EEG signals, respectively, and fused the ECG signals for the binary classification prediction (without motion sickness = 0, with motion sickness = 1). The end-to-end architecture allowed the model to learn optimal feature representations directly from the raw data, enhancing both the sensitivity and interpretability of the features related to motion sickness while providing a reliable basis for analyzing the effect of lighting intervention.

The overall architecture of the passenger motion sickness binary classification model, which contained EEG, ECG data input, temporal convolution module (TCM) of EEG, spatial convolution module (SCM), multi-attention module (AM), ECG feature extraction, fusion module, and finally binary classification recognition, shown in Figure 1. The EEG input is $X_{EEG} \in \mathbb{R}^{B\times T\times C}$, where B is the batch size, T = 256 (2 s 128 Hz), and channel $C = 14$ channels; the ECG input is $X_{ECG} \in \mathbb{R}^{B\times F}$, and F is the ECG feature.

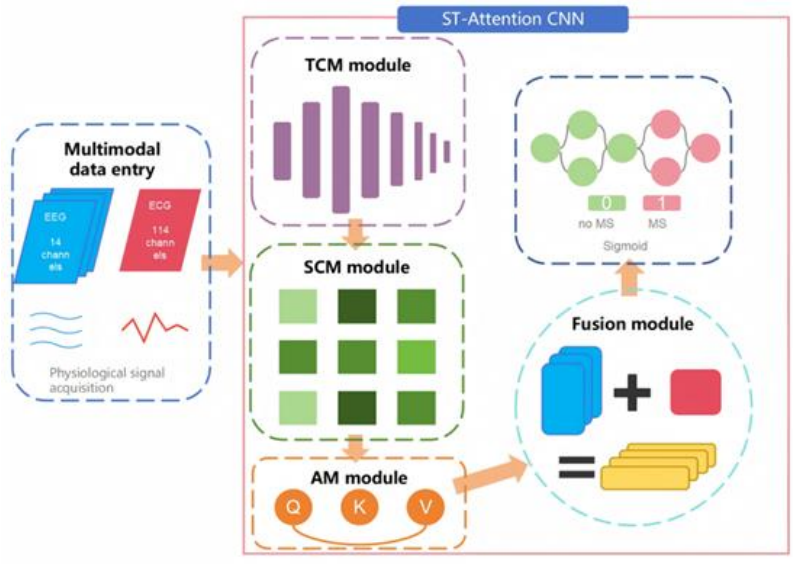

Figure 1. Structure of EEG and ECG fusion model.

The Time Convolution Module (TCM) was designed to capture the temporal dynamics of the EEG signal, which was acquired at a sampling rate of 128 Hz, with a 2-second time window corresponding to 256-time steps and 14 channels constituting an input shape of (256,14) The TCM used a one-dimensional convolution (Conv1D) to extract local patterns in the time dimension and expanded the receptive field to capture features over a more extended period through a dilated convolution (Dilated Convolution). The TCM module contained two layers of 1D Convolution. The mathematical expression of the convolution operation was as follows:

$$h_t^l = \mathrm{ReLU}(\mathrm{BN}(\sum_{i=0}^{k-1} W_i^l \cdot x_{t+i\cdot c}^{l-1} + b^l)) \tag{1}$$

Where was the output of the first-time step of the first layer. The output of the TCM module was shaped as (128,32), where the time step length was halved, and the number of feature channels was increased to 32.

The Spatial Convolution Module (SCM) module was designed to capture the inter-channel spatial correlation of the EEG signal. The TCM output was reshaped as (128,32,1), which treated as a 2D feature map (time step × feature channel × 1), and subsequently, a 2D convolution (Conv2D) was applied to extract the spatial features. The SCM module consists of convolutional and pooling layers. Convolutional Layer: 2D convolution with a convolution kernel of size (3,3) Outputs 16 channels with batch normalization and ReLU activation. Pooling layer: MaxPooling2D, pooling window is (2,2), output shape is reduced from (128,32,16) to (64,16,16). The mathematical expression for the 2D convolution operation is:

$$h_{i,j}^l = \mathrm{ReLU}(\mathrm{BN}(\sum_{m=0}^{k-1}\sum_{n=0}^{k-1} W_{m,n}^l \cdot x_{i+m,j+n}^{l-1} + b^l)) \tag{2}$$

Where $h_{i,j}^l$ is the layer's output at position, $W_{m,n}^l$ is the convolutional kernel weight, and $x_{i+m,j+n}^{l-1}$ is the input feature values. The SCM output shape is (64,16,16), denoting 64-time steps and 16 spatial feature channels.

The Attention Mechanism Module (AM) module enhanced the model's ability to pay attention to key features through the Multi-Head Attention, MHA mechanism. The SCM outputs were fed into the MHA to compute the correlation between the features and generate the attention weights. The formula for calculating Multi-Head Attention was as follows:

$$\text{Attention}(Q, K, V) = \text{softmax}(\frac{QK^T}{\sqrt{d_k}})V \tag{3}$$

$$\text{MultiHead}(Q, K, V) = \text{Concat}(\text{head}_1, \text{head}_2, \ldots, \text{head}_h)W^O \tag{4}$$

Where is the Query, Key, and Value, respectively, generated from the SCM output by linear transformation; d_k is the dimension of the key; and is the W^O output projection matrix. ECG features vary through the fully connected layer.

$$h_{ECG} = \text{ReLU}(X_{ECG}W^{ECG} + b^{ECG}) \tag{5}$$

The following steps performed subsequent binary prediction: Fully connected layer: 64 neurons, ReLU activation, L2 regularization (coefficient 0.005); Dropout: 0.4 to prevent overfitting; Output layer: 1 neuron, Sigmoid activation for classification (no motion sickness = 0, motion sickness = 1). The mathematical expression of the Sigmoid activation function was as follows:

$$p = \frac{1}{1 + e^{-z}} \tag{6}$$

Where z is the logits value of the output layer; p is the predicted probability of 'having motion sickness' (category 1). The model uses a binary cross-entropy loss function defined as follows:

$$\mathcal{L} = -\frac{1}{N}\sum_{i=1}^{N}[y_i \log(\hat{y}_i) + (1 - y_i)\log(1 - \hat{y}_i)] \tag{7}$$

Where N is the number of samples; y_i is the true label (0 or 1); and $\hat{y}_i$ is the predicted probability.

3. Experimental design and subjective analysis

3.1. Experimental design

The experiment was conducted with Feifan F7 series electric vehicles on a fixed route (12.1 km long, covering the Outer Ring Road, S7 Expressway, Bao'an Highway to Hutai Road) in Baoshan District, Shanghai. The route contains city roads, highways, and complex road conditions, simulating real driving scenarios to ensure the external validity of the results. The vehicle was equipped with an adjustable ambient lighting system, and the experimental process and roads was shown in Figure 2. Three lighting conditions were set for the experiment: (1) cool blue light (wavelength 450–470 nm); (2) Warm-toned red light (wavelength 620–650nm); (3) No light control group (ambient light intensity < 5 lux).

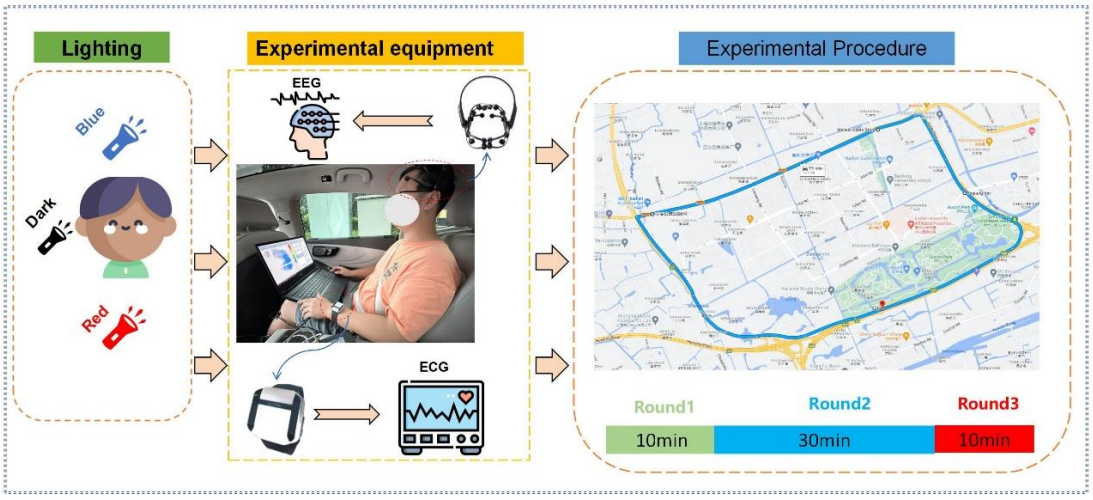

Figure 2. Flow chart of real vehicle experiment.

This experiment was conducted on a fixed circular actual roadway, and all tests were conducted at night (20:00 pm–24:00 pm) to simulate a nighttime driving environment. Each group of experiments was conducted for 50 minutes (10 minutes resting, 30 minutes real vehicle experiment, 10 minutes recovery). The test route was located near Gucun Park in Baoshan District, Shanghai, and the circular route of the test contained urban sections and highways. Inside the car, in addition to the experimental lights off the instrument panel, the center control screen, and other potential interference light sources. The real vehicle environment for nighttime lighting intervention was shown in Figure 3.

Figure 3. Lighting intervention in the real vehicle environment at night.

Three healthy male volunteers were recruited for this experiment, and each subject was tested under each of the three lighting conditions (red, blue, and dim), totaling nine sets of data (3 subjects × three conditions). The data for each condition were derived from the subjective motion sickness scores of the same subject in the corresponding lighting environment, recorded over 30 minutes at 5-minute intervals, for a total of 54 scores. The subjective motion sickness scores of the participants were assessed using the Quick Motion Sickness Scale, as presented in Table 1.

Table 1. Quick motion sickness scale.

Score	Description
1	No Motion Sickness: The participant experiences no symptoms of motion sickness and feels normal.
2	Mild Motion Sickness: The participant experiences mild motion sickness but is still able to continue normal activities.
3	Some Motion Sickness: The participant experiences symptoms of motion sickness, such as mild discomfort, but is still able to continue normal activities.
4	Severe Motion Sickness: The participant experiences moderate symptoms of motion sickness, such as dizziness and nausea, which affect their ability to continue normal activities.
5	Extremely Severe Motion Sickness: The participant experiences severe motion sickness symptoms, such as intense dizziness and nausea, and is unable to continue normal activities.
6	Unbearable Motion Sickness: The participant experiences extremely severe symptoms, such as unbearable dizziness, nausea, and vomiting, requiring immediate cessation of activity and medical attention.

3.2. Subjective analysis

In order to facilitate the dichotomous analysis, the motion sickness scores were converted into dichotomous labels: a score value of 1 was defined as "no motion sickness" (category 0), and a score value greater than 1 was defined as "motion sickness" (category 1), shown in Table 2.

Table 2. Classification and distribution of motion sickness.

Lighting conditions	No motion sickness (0)	With motion sickness (1)	(grand) total
dark light	5	13	18
blue light	7	11	18
red light	14	4	18
total	26	28	54

The proportion of motion sickness without motion sickness under red light conditions was the highest, at 77.8% (14/18), and the proportion of motion sickness was only 22.2% (4/18), indicating that red light has a significant effect on relieving motion sickness. The proportion of motion sickness under dark light conditions was the highest, at 72.2% (13/18), and the proportion of motion sickness without motion was only 27.8% (5/18), indicating that dark light may aggravate the feeling of motion sickness. The distribution of motion sickness under blue light conditions was relatively balanced, with the proportion of motion sickness without motion sickness being 38.9% (7/18), and the proportion of motion sickness being 61.1% (11/18), reflecting a moderate tendency to motion sickness.

In order to quantify the subjective feelings of motion sickness scores, the mean (M) and standard deviation (SD) of the original scores under each lighting condition were calculated. The mean motion sickness scores under red light conditions were the lowest (M = 1.222, SD = 0.428), and the standard deviation was the smallest; the mean motion sickness scores under dark light conditions were the highest (M = 2.278, SD = 0.894), with a large standard deviation, indicating a heavy motion sickness feeling and obvious differences between individuals; the mean motion sickness scores under blue light conditions were centered (M = 1.833, SD = 0.786), and the standard deviation was between the two, reflecting moderate degree of motion sickness feeling and individual differences.

In order to examine the significant effect of lighting conditions on the distribution of motion sickness, a chi-square test was used for analysis. The difference between the observed and expected frequencies could calculate the chi-square statistics.

$$\chi^2 = \sum \frac{(O - E)^2}{E} \tag{8}$$

According to the data of Table 3, the chi-square value was 9.94, the degree of freedom was 2, and the p-value is less than 0.01, indicating that the influence of lighting conditions on the distribution of motion sickness categories is statistically significant.

Table 3. Mean and standard deviation of subjective motion sickness scores conditions.

Lighting conditions	Sample size (n)	Mean (M)	Standard deviation (SD)
dark light	18	2.278	0.894
blue light	18	1.833	0.786
red light	18	1.222	0.428

4. Statistical analyses of physiological indicators

4.1. EEG feature analysis

The electroencephalogram (EEG) device used a 14-channel electroencephalogram monitor (sampling rate 128 Hz). It was arranged according to the International 10–20 system to monitor the frontal, parietal, and occipital lobe areas to analyze the impact of the lighting environment on brain neural activity. The raw EEG signals underwent preprocessing steps including bandpass filtering (0.5–50 Hz) to remove baseline drift and high-frequency noise, notch filtering (50 Hz) to eliminate power line interference, and artifact removal using independent component analysis (ICA) to eliminate eye movement and muscle artifacts. The extracted features included delta_power (0.5–4 Hz), theta_power (4–8 Hz), alpha_power (8–13 Hz), and delta/alpha ratio. The Table 4 listed the mean and standard deviations of EEG characteristics under three lighting conditions, calculated based on 18 measurements (54 times in total) of each subject in each lighting environment.

Table 4. Mean and standard deviation of EEG characteristics.

Lighting conditions	delta_power	theta_power	alpha_power	delta/alpha
dark light	0.320 ± 0.113	0.079 ± 0.080	0.050 ± 0.034	56.136 ± 122.372
blue light	0.323 ± 0.045	0.049 ± 0.043	0.058 ± 0.026	24.451 ± 32.360
red light	0.292 ± 0.084	0.059 ± 0.040	0.092 ± 0.075	24.802 ± 27.685

According to the EEG characteristic analysis in Table 4, the mean value of the delta_power under blue light conditions was the highest (0.323), the second was dark light (0.320), the lowest was red light (0.292), and the maximum standard deviation of the dark light (0.113).

We repeated measurement ANOVA calculation used to test the main effect of lighting conditions on EEG characteristics. The calculation formula is as follows:

$$M_{total} = \frac{\sum X_{ij}}{N} \tag{9}$$

Where X_{ij} is the jth observation value of the ith group, and N is the total number of observations.

Sum of squares between groups:

$$SSB = n\sum(M_i - M_{total})^2 \tag{10}$$

Where n is the number of data points per group; M_i is the mean of the ith group.

Sum of squares within the group:

$$SSW = \sum(X_{ij} - M_i)^2 \tag{11}$$

Where X_{ij} is the jth observation value of the ith group.

Inter-group mean square MSB and intra-group mean square MSW:

$$\begin{cases} MSB = \dfrac{SSB}{df_B} \\ MSW = \dfrac{SSW}{df_W} \end{cases} \tag{12}$$

Where df_B is the degree of freedom between groups ($df_B = k - 1$), k is the number of experimental groups; df_W is the degree of freedom within groups ($df_W = N - k$).

F value calculation:

$$F = \frac{MSB}{MSW} \tag{13}$$

We repeated measurements of ANOVA test the main effect of lighting conditions on EEG characteristics, shown in Table 5.

Table 5. EEG repeated measurement ANOVA results.

EEG features	F	p	Significance ($p < 0.05$)
delta_power	60.59	< 0.001	Significant
theta_power	101.94	< 0.001	Significant
alpha_power	308.00	< 0.001	Significant
delta/alpha	88.36	< 0.001	Significant

The results showed that all EEG characteristics significantly differ under different lighting conditions ($p < 0.05$). The highest F value of alpha_power (308.00) indicated that the lighting conditions have the most significant impact on the alpha wave power. The F values of theta_power and delta_power was 101.94 and 60.59, respectively, showing the significant regulatory effect of light on low-frequency activity in the brain. The differences between the groups were further analyzed using paired t-test (paired sample t-test). This study used Bonferroni correction to control the false positive risk caused by multiple comparisons.

The formula for calculating the t value:

$$t = \frac{M_1 - M_2}{\sqrt{\dfrac{MSW}{n}}} \tag{14}$$

Among them, M_1 and M_2 are the mean of the two groups, and n is the number of samples, in Table 6.

Table 6. Post-hoc t-test results for EEG signatures.

EEG features	contrast	t	p	Significance（p < 0.05）
delta_power	Blue *vs.* Red	12.87	< 0.001	Significant
	Blue *vs.* Dark	1.42	0.157	Not significant
	Red *vs.* Dark	–9.36	< 0.001	Significant
theta_power	Blue *vs.* Red	–5.09	< 0.001	Significant
	Blue *vs.* Dark	–10.61	< 0.001	Significant
	Red *vs.* Dark	–7.93	< 0.001	Significant
alpha_power	Blue *vs.* Red	–19.11	< 0.001	Significant
	Blue *vs.* Dark	7.36	< 0.001	Significant
	Red *vs.* Dark	18.50	< 0.001	Significant
delta/alpha	Blue *vs.* Red	0.68	0.497	Not significant
	Blue *vs.* Dark	–9.69	< 0.001	Significant
	Red *vs.* Dark	–9.84	< 0.001	Significant

The t-test results showed that delta_power differs significantly between blue and red light (t = 12.87), and the contrast between red and dark light showed a negative t value (t = −9.36), indicating that delta_power is significantly lower than dark light under red light, which is related to red light relieving motion sickness; theta_power is the most obvious difference between blue and dark light (t = −10.61, p = 2.18e−25), and dark light may aggravate the activity of theta waves and reflect stronger motion sickness-related neural responses; alpha_power has the highest t value in red and dark light (t = 18.50, p = 8.56e−69), and the average of alpha_power under red light (0.092), which may promote relaxation by enhancing alpha waves, thereby alleviating motion sickness symptoms.

4.2. ECG feature analysis

Electrocardiogram (ECG) characteristics included mean heart rate (avg_hr), heart rate variability indicators (sdnn, rmssd), and low-frequency/high-frequency ratio (lf_hf). The raw ECG signals were preprocessed using bandpass filtering (0.5–40 Hz) to remove baseline wander and high-frequency noise, followed by R-peak detection algorithms to identify cardiac cycles and calculate R-R intervals. Heart rate variability (HRV) parameters were then computed from the R-R interval time series. Due to the lf_hf data exception, only avg_hr, sdnn and rmssd were analyzed in Table 7. Repeated measurements of ANOVA were used to test the main effect of lighting conditions on ECG characteristics, shown in Table 8.

Table 7. Mean and standard deviation of ECG characteristics.

Lighting conditions	avg_hr (bpm)	SDNN (ms)	RMSSD (ms)
Dark light	61.525 ± 21.221	7.057 ± 23.874	27.211 ± 46.883
Blue light	61.642 ± 24.079	7.300 ± 20.778	30.816 ± 42.998
Red light	61.631 ± 22.322	7.627 ± 22.876	31.302 ± 46.075

Table 8. ECG repeated measures ANOVA results.

ECG Features	F	p	Significance (p < 0.05)
avg_hr	0.01	0.988	Not significant
sdnn	0.23	0.791	Not significant
rmssd	1.15	0.316	Not significant

The results showed that the lighting conditions have no significant effect on avg_hr, sdnn and rmssd ($p > 0.05$). The F value of avg_hr was the lowest (0.01, $p = 0.988$), indicating that the heart rate has almost no change under different lighting conditions; the F values of sdnn and rmssd was 0.23 and 1.15, respectively (p values are 0.791 and 0.316, respectively), indicating that the effect of lighting conditions on heart rate variability is not significant. Bonferroni correction was also used to control the false positive risk caused by multiple comparisons, shown in Table 9.

Table 9. Post-hoc t-test results for EEG characteristics.

ECG Features	Comparison	t	p	Significance（p < 0.0167）
avg_hr	Blue *vs.* Red	0.04	0.968	Not significant
	Blue *vs.* Dark	0.15	0.883	Not significant
	Red *vs.* Dark	0.09	0.926	Not significant
sdnn	Blue *vs.* Red	−0.03	0.978	Not significant
	Blue *vs.* Dark	0.62	0.535	Not significant
	Red *vs.* Dark	0.61	0.542	Not significant
rmssd	Blue *vs.* Red	0.26	0.795	Not significant
	Blue *vs.* Dark	1.37	0.173	Not significant
	Red *vs.* Dark	1.14	0.256	Not significant

In order to reduce feature redundancy and improve the efficiency of the passenger motion sickness binary classification model, Pearson correlation analysis was used to screen features highly correlated with motion sickness status. The analysis was based on 54 sets of data covering EEG and ECG characteristics. Figure 4 showed the feature correlation heat map.

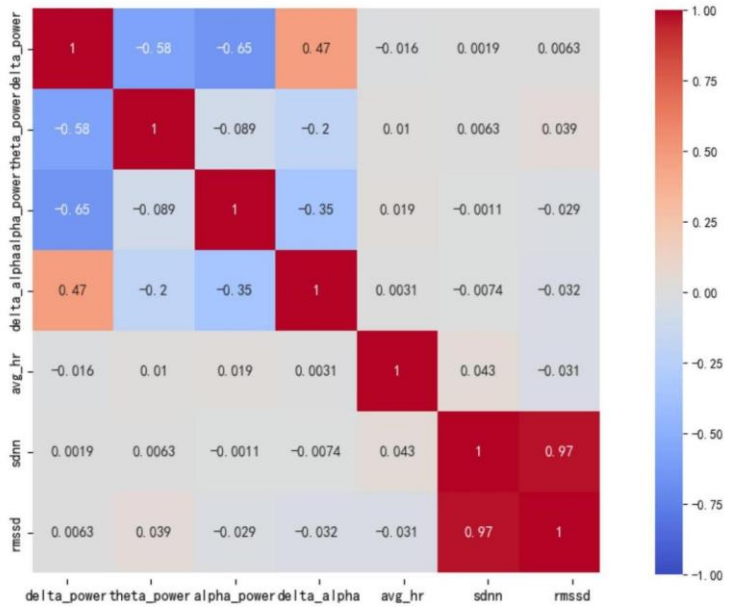

Figure 4. Feature correlation heat map.

5. Performance evaluation of motion sickness model

This section evaluated the performance of passenger motion sickness binary classification models in motion sickness binary classification (0 = no motion sickness, 1 = having motion sickness) taskes through Accuracy, MacroF1-score, and Confusion Matrix and compares them with other machine learning models. The experiment was based on multimodal physiological signals (EEG and ECG features), labeled as the binary classification results of subjective motion sickness scores. Through analysis, the prediction ability of EEG and ECG fused in a night vehicle-mounted environment was verified to provide data support for the effect of lighting intervention.

The experimental data was derived from physiological signals and subjective motion sickness scores of three healthy male subjects under three lighting conditions (dark, blue, and red light) and nine sets of data (3 subjects × 3 conditions). Each data set contains 30 minutes of EEG and ECG signals, and a motion sickness score was recorded every 5 minutes (6 scores in total). The EEG signal was collected at a sampling rate of 128 Hz and contains 14 channels; the ECG signal was collected at a sampling rate of 40 Hz and contains one channel.

Model performance evaluation indicators included accuracy and macroF1-score. The specific results of each model was shown in Table 10 below. The passenger motion sickness classical model performed best in accuracy and macro-average F1 scores, at 0.925 and 0.924, respectively, significantly better than other models. Logistic regression was second, with an accuracy rate of 0.83 and a macro F1 score of 0.86. XGBoost's macro F1 score was higher (0.85) but slightly lower accuracy (0.77). Naive Bayes performed the worst, with an accuracy rate of only 0.60 and a macro F1 score of 0.63, probably due to its characteristic independence assumption that does not apply to the complex correlations of EEG and ECG signals.

Table 10. Evaluation indexes of each model.

Model	Accuracy	Macro average F1-score
SVM	0.80	0.83
XGBoost	0.77	0.85
RF	0.80	0.80
LR	0.83	0.86
NB	0.60	0.63
EEG and ECG Fusion	0.925	0.924

The confusion matrix further analyzed EEG and ECG fusion classification performance, as shown in Figure 5. The matrix showed that the model has excellent classification effects on "free motion sickness" (category 0) and "having motion sickness" (category 1) and correctly predicted 1326 and 1652 samples, with fewer misclassified samples (category 0 misclassified 98, and category one misclassified 143), indicating that the model can effectively distinguish motion sickness status.

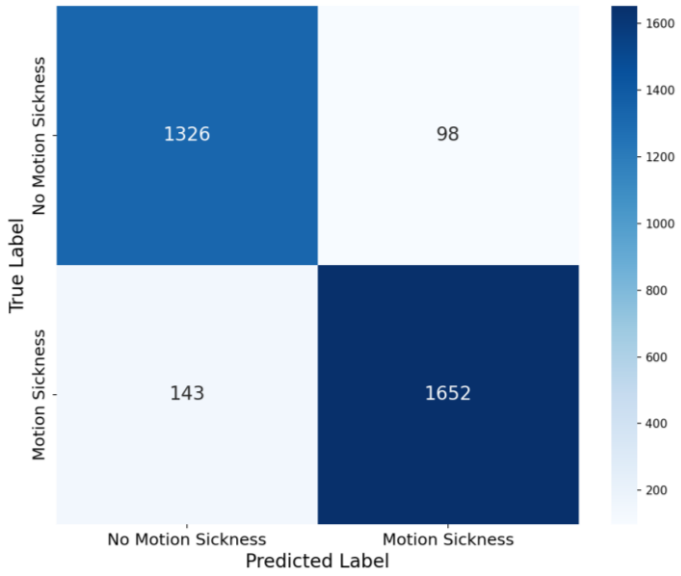

Figure 5. Confusion matrix for EEG and ECG fusion.

The findings of this study demonstrated the potential of wavelength-specific ambient lighting, particularly warm red light, to mitigate passenger motion sickness during nighttime driving. The EEG-ECG fusion model achieved high accuracy (92.5%) and macro F1-score (92.4%), outperforming traditional machine learning models such as SVM, XGBoost, RF, LR and NB. These results demonstrated that the integration of multimodal physiological signals (EEG and ECG) could provide a robust approach for detecting motion sickness, with red light significantly enhancing alpha power and reducing delta power, indicative of neurological relaxation. The superior performance of the fusion model highlights its capability to capture complex correlations in physiological data, offering a promising tool for real-time motion sickness monitoring in intelligent vehicle cabins.

6. Conclusion

In this study, by systematically evaluating the effects of different lighting conditions on motion sickness in a real vehicle environment, we confirmed the significant effect of warm red light (620–650 nm) in alleviating motion sickness, with a significantly lower motion sickness score (mean 1.22) than that of the blue light condition (1.83) and the dark control group (2.78), and the analysis of physiological mechanisms indicated that red light exerts a neuro relaxation effect by reducing delta power (0.292), enhanced alpha power (0.092) and reduced delta/alpha ratio (24.802) to exert a neuro relaxation effect. The dichotomous motion sickness classification model developed based on EEG and ECG multimodal physiological signals achieved a classification accuracy of 92.5% and a macro F1 score of 92.4%.

The main contribution of this study included verifying the mitigating effect of red light on passenger motion sickness and analyzing its neurophysiological mechanism, constructing a binary classification model for passenger motion sickness based on physiological signals, and proposing an adaptive lighting intervention strategy to enhance the passengers' comfort.

The study also underscored the importance of preprocessing techniques, such as bandpass filtering and SMOTE, in addressing signal noise and class imbalance, which enhanced the model's predictive accuracy. In future, we will explore the long-term effects of ambient lighting on motion sickness and to refine the

fusion model's performance under varied driving conditions. These advancements could facilitate the integration of such systems into intelligent vehicle cabins, enhancing passenger comfort and safety.

Acknowledgments

The authors appreciate for the support from the cooperating company, SAIC Motor R&D Innovation Headquarters, SAIC Motor Corporation Limited, Shanghai 201804, China. The authors also express sincere gratitude to the SAIC colleagues Peng Qiu, Tenglong Zhang, Shuang Wang and Bin Wang. This research was funded by the National Natural Science Foundation of China (Grant No. 51775325); Joint Funds of the National Natural Science Foundation of China (Grant No. U21A20121); Key Research and Development Program of Ningbo (Grant No. 2023Z218). The study was conducted according to the guidelines of the Declaration of Helsinki and approved by the Academic Ethics Committee of Shanghai University (2022-011), data of approval: 22 February 2022.

Authors' contribution

Conceptualization, B.R. and X.W.; methodology, B.R. and X.W.; data acquisition, X.W. and P.R.; data analysis and interpretation, B.R. and X.W.; writing—original draft preparation, X.W.; writing—review and editing, B.R., P.R. and M.W; funding acquisition, B.R. All authors have read and agreed to the published version of the manuscript.

Conflicts of interests

The authors declare no conflict of interest.

References

[1] Golding JF. Motion sickness. *Handb. Clin. Neurol.* 2016, 137:371–390.

[2] Iskander J, Attia M, Saleh K, Nahavandi D, Abobakr A, *et al*. From car sickness to autonomous car sickness: a review. *Transp. Res. F: Traffic Psychol. Behav.* 2019, 62:716–726.

[3] Lackner JR. Motion sickness: more than nausea and vomiting. *Exp. Brain Res.* 2014, 232(8):2493–2510.

[4] Schmidt EA, Kuiper OX, Wolter S, Diels C, Bos JE. An international survey on the incidence and modulating factors of carsickness. *Transp. Res. F: Traffic Psychol. Behav.* 2020, 71:76–87.

[5] Tadese Z, Teshome B, Mengistu E. Factors affecting car sickness of passengers traveled by vehicles in North Shewa Zone, Oromia, Ethiopia. *J. Environ. Public Health* 2022, 2022(1):6642603.

[6] Turner M. Motion sickness in public road transport: passenger behaviour and susceptibility. *Ergonomics* 1999, 42(3):444–461.

[7] Wibirama S, Wijayanto T, Nugroho HA, Bahit M, Winadi MN. Quantifying visual attention and visually induced motion sickness during day-night driving and sleep deprivation. In *2015 International Conference on Data and Software Engineering (ICoDSE)*, Yogyakarta, Indonesia, November 25–26, 2015, pp. 191–194.

[8] Wood JM. Nighttime driving: visual, lighting and visibility challenges. *Ophthalmic Physiol. Opt.* 2020, 40(2):187–201.

[9] Bridgeman B, Blaesi S, Campusano R. Optical correction reduces simulator sickness in a driving environment. *Hum. Factors* 2014, 56(8):1472–1481.

[10] Weisgerber DM, Nikol M, Mistlberger RE. Driving home from the night shift: a bright light intervention study. *Sleep Med.* 2017, 30:171–179.

[11] Diels C, Dugenetet P, Brietzke A, Xuan RP. Design strategies to alleviate motion sickness in rear seat passengers—a test track study. In *2023 IEEE 26th International Conference on Intelligent Transportation Systems (ITSC)*, Bilbao, Spain, September 24–28, 2023, pp. 5254–5258.

[12] Keshavarz B, Hecht H. Validating an efficient method to quantify motion sickness. *Hum. Factors* 2011, 53(4):415–426.

[13] Hainich R, Drewitz U, Ihme K, Lauermann J, Niedling M, *et al*. Evaluation of a human–machine interface for motion sickness mitigation utilizing anticipatory ambient light cues in a realistic automated driving setting. *Information* 2021, 12(4):176.

[14] Kim K, Hirayama K, Yoshida K, Yano R, Abe M, *et al*. Effect of exposure to short-wavelength light on susceptibility to motion sickness. *Neuroreport* 2017, 28(10):584–589.

[15] Antemie RG, Samoilă OC, Clichici SV. Blue light—ocular and systemic damaging effects: a narrative review. *Int. J. Mol. Sci.* 2023, 24(6):5998.

[16] Litscher D, Wang L, Gaischek I, Litscher G. The influence of new colored light stimulation methods on heart rate variability, temperature, and well-being: results of a pilot study in humans. *Evid. Based Complement Alternat. Med.* 2013, 2013(1):674183.

[17] Mao Y, Pan L, Li W, Xiao S, Qi R, *et al*. Stroboscopic lighting with intensity synchronized to rotation velocity alleviates motion sickness gastrointestinal symptoms and motor disorders in rats. *Front. Integr. Neurosci.* 2022, 16:941947.

[18] Henry EH, Bougard C, Bourdin C, Bringoux L. Changes in electroencephalography activity of sensory areas linked to car sickness in real driving conditions. *Front. Hum. Neurosci.* 2022, 15:809714.

[19] Li C, Zhang Z, Liu Y, Zhang T, Zhang X, *et al*. Multi-dimensional and objective assessment of motion sickness susceptibility based on machine learning. *Front. Neurol.* 2022, 13:824670.

[20] Keshavarz B, Peck K, Rezaei S, Taati B. Detecting and predicting visually induced motion sickness with physiological measures in combination with machine learning techniques. *Int. J. Psychophysiol.* 2022, 176:14–26.

[21] Irmak T, Pool DM, Happee R. Objective and subjective responses to motion sickness: the group and the individual. *Exp. Brain Res.* 2021, 239(2):515–531.